J Biol Phys (2008) 34:425–432
DOI 10.1007/s10867-008-9069-0

ORIGINAL PAPER

Wave-Block Due to a Threshold Gradient Underlies Limited Coordination in Pancreatic Islets

Morten Gram Pedersen · Mads Peter Sørensen

Received: 11 January 2008 / Accepted: 21 March 2008 /
Published online: 13 May 2008

Abstract Two models for coupled pancreatic β cells are used to investigate excited wave propagation in spatially inhomogeneous islets of Langerhans. The application concerns spatial variation of glucose concentration across the islet. A comprehensive model of coupled cells shows that wave blocking occurs as the conductance of adenosine triphosphate regulated potassium channels increases, corresponding to spatially decreasing glucose concentration. A simplified model based on a perturbed version of Fisher's equation has been investigated using perturbation theory. We show that the perturbed Fisher's equation likewise can exhibit wave blocking.

Keywords Calcium waves · Propagation failure · Nonlinear excitation waves · Inhomogeneous media

1 Introduction

Malfunctioning of the insulin secretory system is a major factor in diabetes. The pancreatic islets of Langerhans consist of thousands of coupled cells; among these are the β cells, which secrete insulin in response to several stimuli, with glucose being the physiologically most important. In order to function properly and secrete insulin, it is of great importance

M. G. Pedersen
Department of Information Engineering, University of Padova,
Via Gradenigo, 6/B, 35131 Padova, Italy

M. G. Pedersen
Department of Physics, Technical University of Denmark,
Fysikvej, Bldg. 309, 2800 Kgs. Lyngby, Denmark

M. P. Sørensen (✉)
Department of Mathematics, Technical University of Denmark,
Matematiktorvet, Bldg. 303S, 2800 Kgs. Lyngby, Denmark
e-mail: M.P.Soerensen@mat.dtu.dk

that the β cells cooperate in a synchronized manner, and the coupling between cells made of gap junctions seems to be crucial for this synchronization ([1–3] and references herein).

An increased intracellular calcium concentration is the signal that triggers insulin release, and thus, synchronized insulin secretion would be expected to be a result of synchronized Ca^{2+} levels. In [4], it was shown experimentally that calcium waves could provide a way to synchronize the cells. Using a mathematical model of β cells, the authors showed that gap junctions indeed could result in waves of the observed kind. Moreover, it was suggested that active cells could activate less responsive cells by means of the waves.

In an elegant experiment [5], it was shown that such an activation signal from active to silent cells is only able to travel short distances. The authors imposed a glucose gradient across an islet such that cells in one part of the islet would feel a glucose concentration high enough to promote calcium influx and insulin secretion, while the rest of the islet sensed a lower glucose stimulus, below the activation threshold. Calcium wave propagation starting from the cells in high glucose was seen, but these waves did not travel into the region with a glucose concentration below the threshold, activating none or, at most, very few of the otherwise silent cells. In this article, we shall elucidate these findings, invoking mathematical modelling of pancreatic β cells.

2 Mathematical Models and Fisher's Equation

Almost all mathematical models of β cell electrical activity and calcium dynamics are of the form

$$\frac{dv}{dt} = -I(v, n, s) \ , \tag{1}$$

$$\frac{dn}{dt} = \frac{n_\infty(v) - n}{\tau_n} \quad \text{and} \quad \frac{ds}{dt} = \frac{s_\infty(v) - s}{\tau_s} \ , \tag{2}$$

where $v = v(t)$ models the membrane potential as function of time t, and $n = n(t)$ and $s = s(t)$ are fast and slow gating variables, respectively, i.e., $\tau_n \ll \tau_s$. I is the sum of the ion currents flowing through the cell membrane gates [6]. It has been argued that, on the front of an excitation wave, we can assume $n = n_\infty(v)$ and $s = s^*$ to be constant [4]. Then, (1) becomes

$$\frac{dv}{dt} = -I(v, n_\infty(v), s^*) = F(v; s^*) \ , \tag{3}$$

where $F = F(v; s^*)$ has three simple zeros $v_0 < v_a < v_1$ and is negative on the interval $]v_0; v_a[$. When we consider a line of N coupled cells, this becomes

$$\frac{dv_i}{dt} = F(v_i; s_i^*) + g_c(v_{i+1} - 2v_i + v_{i-1}), \quad i = 1, \ldots, N \ , \tag{4}$$

where i counts the cells. We use open-end boundary conditions equivalent to $v_0 = v_1$, $v_{N+1} = v_N$. The coupling between cells is due to gap junctions and we assume a resistive ion current coupling with conductivity g_c. The continuum limit of the discrete equation (4) yields [4]

$$v_t = F(v; s) + D v_{xx} \ .$$

Here, subscripts denote differentiation with respect to the subscript variable. Note that s is allowed to be a function of x. After a suitable change of variables (see [7] for details), this equation can be transformed into Fisher's equation

$$u_t = f(u; a) + u_{xx} \,, \tag{5}$$

where $f = f(u; a)$ has three simple zeros when varying the variable u, for the parameter a belonging to the interval $0 < a < 1$ and $f(u; a)$ is negative for $u \in [0; a]$. The prototype is the cubic $f(u) = u(1-u)(u-a)$. It is well known [8, 9] that, for constant $a = a_0$ and $\int_0^1 f(u; a)du > 0$, (5) has a traveling wave solution

$$u(x, t) = U(x - vt) = U(\xi) = \frac{1}{1 + \exp(\xi/\sqrt{2})} \,, \tag{6}$$

where $\xi = x - vt$ with $\lim_{\xi \to -\infty} U(\xi) = 1$, $\lim_{\xi \to \infty} U(\xi) = 0$, and $v = (1-2a)/\sqrt{2}$. This means the solution has a kink shape.

The present work investigates the experiments described in [5] with a glucose gradient across the islet following the ideas above. Because an imposed glucose gradient corresponds to the threshold changing across the islet, we perturb the threshold a in (5), as well as the equation itself:

$$u_t = f(u; a) + u_{xx} + \epsilon g(x), \qquad a = a_0 + \epsilon a_1(x) \,, \tag{7}$$

where we require $0 < a < 1$ and a_1 and g sufficiently smooth. Using perturbation theory much in the spirit of Keener's investigation of the homogenized equation (5) [8], we show that a space varying parameter $a = a(x)$ leads to a change in the propagation velocity v of the kink type solution in (6). This may result in a halt of the wave (wave blocking). We conjecture that a varying $a(x)$ can model a glucose gradient through an islet of Langerhans leading to the observed wave block phenomena observed experimentally in [5].

3 Wave Propagation and Wave Block

We set [8, 9]

$$\xi = x - \phi(t) \,, \quad U(\xi) = u(x, t) \,,$$

such that (7) becomes

$$-\phi'(t)U' = U'' + f(U, a) + \epsilon g \,. \tag{8}$$

In the following, we let $f_u(u, a)$ denote the partial derivative of $f(u, a)$ with respect to u, similarly for $f_a(u, a)$. Introducing

$$U = U_0 + \epsilon U_1 \,,$$
$$\phi'(t) = v_0 + \epsilon \phi_1'(t) \,,$$
$$f(U, a) = f(U_0, a_0) + \epsilon U_1 f_u(U_0, a_0) + \epsilon a_1 f_a(U_0, a_0) + o(\epsilon^2) \,,$$

in (8) and collecting terms with the same order in ϵ yields for ϵ^0 and ϵ^1,

$$-v_0 U_0' = U_0'' + f(U_0, a_0) \,, \tag{9}$$

$$-\phi_1'(t)U_0' - v_0 U_1' = U_1'' + U_1 f_u(U_0, a_0) + a_1 f_a(U_0, a_0) + g. \tag{10}$$

From (9), we see that the zero-order solution U_0 and speed v_0 are given from the standard solution of (5). Equation 10 can then be written

$$\begin{aligned} L[U_1] :&= U_1'' + v_0 U_1' + f_u(U_0, a_0) U_1 \\ &= -\phi_1'(t) U_0' - a_1(\xi + \phi(t)) f_a(U_0, a_0) - g(\xi + \phi(t)) \ . \end{aligned} \tag{11}$$

By differentiating (9) with respect to ξ, we find $L[U_0'] = 0$. The adjoint operator $L^\dagger$ [9], defined by $\langle p(\xi) L\, q(\xi)\rangle = \langle (L^\dagger p(\xi)) q(\xi)\rangle$, then has $L^\dagger[W] = 0$ for $W(\xi) = e^{v_0 \xi} U_0'(\xi)$. Here, $\langle p, q\rangle = \int_{\mathbb{R}} p(\xi) q(\xi) d\xi$. In order to have a solution of (11), we therefore must demand

$$\begin{aligned} 0 &= \langle -a_1 f_a - \phi_1' U_0' - g, W\rangle \\ &= -\langle a_1 f_a, W\rangle - \phi_1' \langle U_0', W\rangle - \langle g, W\rangle \ . \end{aligned} \tag{12}$$

From (12) we obtain

$$\begin{aligned} \phi_1'(t) &= \Phi(\phi) \\ &= \frac{\int_{-\infty}^{\infty} [-a_1(\xi + \phi)\ f_a(U_0(\xi), a_0) - g(\xi + \phi)]\, e^{v_0 \xi}\ U_0'(\xi) d\xi}{\int_{-\infty}^{\infty} U_0'(\xi)^2\, e^{v_0 \xi} d\xi} \ . \end{aligned} \tag{13}$$

Hence, we have an ordinary differential equation (ODE) for the instantaneous position ϕ, or, in other words, the instantaneous velocity ϕ' is given by

$$\phi' = v_0 + \epsilon \Phi(\phi) \ .$$

From this equation, we can find the location ϕ when the wave front stops, that is, at $\phi' = 0$.

3.1 Example

To illustrate the theory introduced above, we look closer at a case where explicit calculation can be done. Let us consider the cubic

$$f(U, a) = U(1 - U)(U - a) \ , \quad \text{for } \ 0 < a < 1 \ ,$$

in (7), and from (6), the solution U_0=$U_0(\xi)$ of (9) becomes

$$U_0(\xi) = \frac{1}{1 + \exp(\xi/\sqrt{2})} \ , \quad \text{where } \ v_0 = \frac{1 - 2a_0}{\sqrt{2}} \ .$$

Note that $U_0(1 - U_0) = -\sqrt{2} U_0'$, so that the denominator of (13) becomes

$$\begin{aligned} K_0 &= \int_{-\infty}^{\infty} (U_0'(\xi))^2 \exp(v_0 \xi) d\xi = -\int_{-\infty}^{\infty} U_0(1 - U_0) \exp(v_0 \xi) U_0' d\xi / \sqrt{2} \\ &= -\int_1^0 U_0(1 - U_0) \left(\frac{1 - U_0}{U_0}\right)^{\sqrt{2} v_0} dU_0 \ / \sqrt{2} \\ &= \int_0^1 U_0^{2a_0} (1 - U_0)^{2 - 2a_0} dU_0 / \sqrt{2} = B(2a_0 + 1, 3 - 2a_0)/\sqrt{2} \ , \end{aligned}$$

where we have used the substitution $\xi = \sqrt{2}\ln\left(\frac{1-U_0}{U_0}\right)$, and introduced the Beta function B. Assume $g = 0$ and

$$a(x) = a_0 + \varepsilon a_1(x) \quad \text{with} \quad a_1(x) = \exp(x/\sqrt{2}) \,, \tag{14}$$

where a_0 is a constant and $\varepsilon \ll 1$. The partial derivative of f with respect to a is $f_a(U_0, a_0) = -U_0(1-U_0)$ and the numerator $K_0\Phi(\phi)$ in (13) becomes

$$\int_{-\infty}^{\infty} a_1(\xi+\phi) f_a e^{v_0\xi} U_0'(\xi) d\xi = -\exp(\phi/\sqrt{2}) B(2a_0, 4-2a_0) \,, \tag{15}$$

from which we calculate, using the properties of the B- and Γ-functions,

$$\begin{aligned}\Phi(\phi) &= -\sqrt{2}\exp(\phi/\sqrt{2})\frac{B(2a_0, 4-2a_0)}{B(2a_0+1, 3-2a_0)} \\ &= -\sqrt{2}\exp(\phi/\sqrt{2})\frac{\Gamma(2a_0)\Gamma(4-2a_0)}{\Gamma(4)}\frac{\Gamma(4)}{\Gamma(2a_0+1)\Gamma(3-2a_0)} \\ &= -\sqrt{2}\exp(\phi/\sqrt{2})\left(\frac{3}{2a_0}-1\right) \,.\end{aligned}$$

This result finally yields the simple ODE for ϕ

$$\phi' = v_0 - \varepsilon\sqrt{2}\exp(\phi/\sqrt{2})\left(\frac{3}{2a_0}-1\right) \,,$$

possessing the analytical solution

$$\phi(t) = -\sqrt{2}\ln\left[\left(1-\frac{c}{v_0}\right)e^{-\frac{v_0}{\sqrt{2}}t} + \frac{c}{v_0}\right] \,, \quad \text{where} \quad c = \varepsilon\sqrt{2}\left(\frac{3}{2a_0}-1\right) \,, \tag{16}$$

for the initial condition $\phi(0) = 0$. In Fig. 1 (left), we show a contour plot of a full numerical simulation of the perturbed Fisher's equation (7) with the space-dependent parameter given by $a(x) = a_0 + \varepsilon\exp((x-50)/\sqrt{2})$ [see (14)] and with the initial conditions given

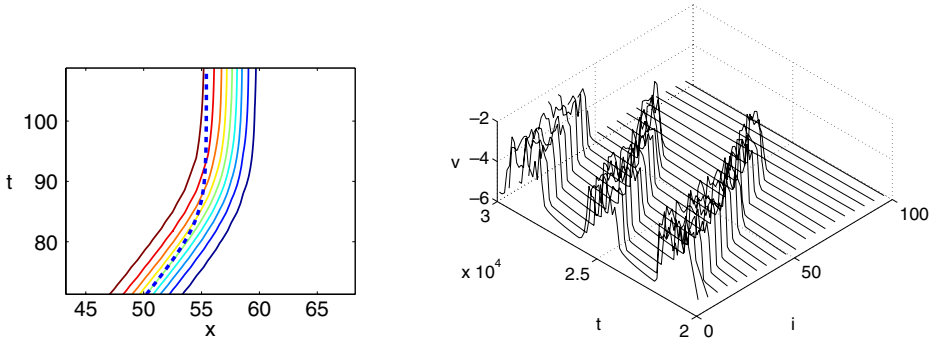

Fig. 1 *Left*: Comparison between the full numerical simulation of the wave block of the perturbed Fisher's equation (7) (*contour plot*) and the approximate solution in (16) (*dashed line*). The parameter values are $a_0 = 0.2$, $\varepsilon = 0.001$, $v_0 = \frac{1-2a_0}{\sqrt{2}} = 0.424$, $g = 0$. *Right*: Simulation of a linear chain of coupled beta cells illustrating wave blocking. The voltage is shown as a function of time and cell position for linearly increasing $g_{K(ATP)}$. Number of cells $N = 100$. Time is measured in units of $k_t = 5.3$ ms and the voltage is measured in units of $k_v = s_m = 12$ mV

by $u(x,0) = 1/(1+\exp((x-20)/\sqrt{2}))$. The perturbation term g is set to zero. From these formulas, we observe that the initial kink is positioned at $x = 20$ and $a(x)$ is "positioned" at $x = 50$. The kink propagation is blocked at position $x \approx 57.7$, a little after the "center position" of $a(x)$. The simulation is compared to the results from the approximation in (16), which provide the trajectory of the kink. The trajectory determined from (16) is shown in Fig. 1 (left) as the dashed line, predicting a wave block at the position $x \approx 55.2$. The approximate analysis predicts a slightly earlier wave block, and also the curvature of the kink trajectory is larger than the results from the full numerical simulation predict. Apart from this, the perturbation analysis seems to give a fair approximation of the full simulation results of (7) with $g = 0$.

4 Wave Block in Coupled Beta Cells: Discrete Model

We now return to the original model of β cell bursting given in (1–2), and this time, we shall be specific about the ion currents I. We consider a model of coupled cells in a line and include an adenosine triphosphate (ATP) regulated calcium gate. Following [6], we consider the model below adapted for coupled β cells

$$c\frac{dv_i}{dt} = -I_{\mathrm{Ca}} - I_{\mathrm{K}} - I_{\mathrm{S}} - I_{\mathrm{K(ATP)}} - \sum_j g_{ij}(v_i - v_j)\ . \tag{17}$$

The notation follows that in (4). The membrane capacitance is denoted by c. The currents I_{Ca} and I_{K} are voltage-dependent inward calcium and outward potassium currents, respectively, which are responsible for fast oscillations during the active phase. The current I_{S} is a slow current responsible for the depolarization of the membrane and $I_{\mathrm{K(ATP)}}$ is an ATP-regulated outward potassium current that is high at low ATP/glucose concentrations and low at high ATP/glucose concentrations, thus describing external control of the ion current activity by glucose metabolism. The final term models the gap junctions, interconnecting nearest neighbor cells, as linear passive electric conductors. The ion currents for cell i are given by [6]

$$I_{\mathrm{Ca}} = g_{\mathrm{Ca}} m_\infty(v_i)(v_i - v_{\mathrm{Ca}})\ , \quad I_{\mathrm{K}} = g_{\mathrm{K}} n(v_i - v_{\mathrm{K}})\ , \tag{18}$$

$$I_{\mathrm{S}} = g_{\mathrm{S}} s(v_i - v_{\mathrm{K}})\ , \quad I_{\mathrm{K(ATP)}} = g_{\mathrm{K(ATP)}}(v_i - v_{\mathrm{K}})\ . \tag{19}$$

The voltage-dependent coefficients $m_\infty(v_i)$, $n = n(v_i, t)$, and $s = s(v_i, t)$ are gating variables controlling the closing and opening of the associated ion channels. The dynamics of the gating variables are governed by (2). Each of the variables m_∞, n_∞, and s_∞ are given by formulas of the same form

$$x_\infty = x_\infty(v_i) = \frac{1}{1+\exp(-(v_i - v_x)/s_x)}\ , \tag{20}$$

where x represents m, n, and s, respectively. Representative parameter values are selected from references [4, 6] and given in Table 1. For the study of the wave front, s can be set to a constant value $s = s^*$, because it is a slow variable, and it can be assumed that the fast-gating variable n attains its equilibrium value $n = n_\infty$. Under these assumptions, the total current then possesses three zeros with the parameter values used here [4], as explained in Section 2. This motivates the study of Fisher's equation in Section 3.1.

With the above model, we are now in a position where we can address the experimental results of wave blocking. A linear glucose gradient was imposed across an islet of

Table 1 Parameter values used in the models

$g_{\mathrm{Ca}} = 1000$ pS	
$v_{\mathrm{Ca}} = 25$ mV	
$v_m = -20$ mV	
$s_m = 12$ mV	
$c = 5300$ fF	
$g_{\mathrm{K}} = 2700$ pS	
$v_{\mathrm{K}} = -75$ mV	
$v_n = -16$ mV	
$s_n = 5.6$ mV	
$\tau_n = 20$ ms	
$g_{\mathrm{s}} = 200$ pS	
$g_{ij} = g_c = 20$ pS	
$v_s = -52$ mV	
$s_s = 5$ mV	
$\tau_s = 20 \times 10^3$ ms	

pS = pico Siemens, mV = millivolt, ms = milliseconds, fF = femto Farad

Langerhans in a microfluidic cavity setup [5]. In our model, this corresponds to varying $g_{\mathrm{K(ATP)}}$ along the cell sites of the linear chain model, and we shall assume a linear spatial variation of $g_{\mathrm{K(ATP)}}$ according to

$$g_{\mathrm{K(ATP)}} = 120 \text{ pS} + (i-1) \cdot 1 \text{ pS}\,, \quad i = 1, 2, 3, \ldots N\,. \tag{21}$$

For single cell dynamics with $g_{ij} = 0$, the model in (17) exhibits continuous spiking for $g_{\mathrm{K(ATP)}} \lesssim 90$ pS, bursting behavior for 90 pS $\leqq g_{\mathrm{K(ATP)}} \leqq 162$ pS, and silence for 162 pS $\lesssim g_{\mathrm{K(ATP)}}$. From (21), we will expect that an excitation wave can propagate along the cell chain from $i = 1$ until, at most, $i \approx 44$. The model equations in (17–19) have been implemented on a computer in a scaled version. Time has been scaled in terms of $k_t = c/g_{\mathrm{Ca}} = 5.3$ ms; that is, time is measured in units of k_t. Similarly, the voltage is scaled according to $k_v = s_m = 12$ mV and, hence, measured in units of k_v. Conductivities are measured in units of $k_g = c/k_t = 1000$ pS. Note that, in (21), we have given the variation of $g_{\mathrm{K(ATP)}}$ in physical units.

We have conducted a simulation in a scaled time interval from $t = 0$ to $t = 3 \cdot 10^4$ (corresponding to 159 s). In Fig. 1 (right), we show the scaled voltage $v_i(t)$ as a function of cell position i and time t for the time interval $t = 2 \cdot 10^4$ (106 s) to $t = 3 \cdot 10^4$ (159 s). The figure shows how fronts form of cells changing from the resting state to the bursting state, and propagate analogous to the front solutions of Fisher's equation (Fig. 1 left). Similarly, we see fronts corresponding to cells changing from the excited state to the silent state. The irregular shape is typically observed in coupled cell dynamics and may be due to chaotic dynamics or irregular synchronisation. At a fixed value of the cell position i less than about 60–80, we observe the characteristic bursting phenomena with decreasing burst period as $g_{\mathrm{K(ATP)}}$ increases as a function of i. For cells at position i larger than about 80, the bursting behavior disappears and the cells are silent. This means we have excitation wave propagation until, at most, cell number 80, and here, wave blocking occurs. We can conclude that the simulation confirms the wave blocking phenomena observed in the experiments from [5].

At cell number 44, the parameter $g_{\mathrm{K(ATP)}}$ equals 163 pS and the single-cell bursting disappears. Therefore, we would expect the excitation wave stops at about $i = 44$. However, the simulations show that the excitation waves propagate further into the region with silent cells leading to an induced bursting of otherwise silent cells. In other words, the coupling

can induce excitation, leading to propagation of an excitation wave further into a region with depleted glucose concentration. This wave penetration is enhanced when increasing the coupling constant $g_{ij} = g_c$.

5 Conclusion

Using mathematical modelling, we have investigated coupled pancreatic β cell dynamics with a focus on inhomogeneous spatial variation of parameters. The purpose is to investigate the occurrence of blocking of excitation waves observed in experiments, where a glucose gradient is imposed across an islet of Langerhans.

An excitation wave can propagate from high glucose concentration toward low glucose concentrations but will be stopped or blocked when entering the low glucose concentration region where the β cells are not excited. Our model shows that wave blocking occurs for spatial variation of the ATP-regulated potassium ion channel gate. In addition, we observe that the gap junction coupling leads to enhanced excitation of otherwise silent cells.

A simplified mathematical model for the wave blocking phenomenon has been suggested in terms of a perturbed Fisher's equation. In the normalized Fisher's equation, there is one parameter a, which gives the propagation velocity of a travelling wave solution. By letting a be a function of space x, perturbation theory shows that increasing a gives rise to blocking of wave propagation.

Acknowledgements We acknowledge financial support from the European Union through the Network of Excellence BioSim, LSHB-CT-2004-005137. MGP was partially supported by the Villum Kann Rasmussen Foundation.

References

1. Eddlestone, G.T., Goncalves, A., Bangham, J.: Electrical coupling between cells in islets of langerhans from mouse. J. Membr. Biol. **77**, 1–14 (1984)
2. Meissner, H.: Electrophysiological evidence for coupling between beta cells of pancreatic islets. Nature **262**(5568), 502–504 (1976)
3. Ravier, M.A., Güldenagel, M., Charollais, A., Gjinovci, A., Caille, D., Sohl, G., Wollheim, C.B., Willecke, K., Henquin, J.C., Meda, P.: Loss of connexin36 channels alters beta-cell coupling, islet synchronization of glucose-induced Ca^{2+} and insulin oscillations, and basal insulin release. Diabetes **54**, 1798–1807 (2005)
4. Aslanidi, O.V., Mornev, O., Skyggebjerg, O., Arkhammar, P., Thastrup, O., Sørensen, M.P., Christiansen, P.L., Conradsen, K., Scott, A.C.: Excitation wave propagation as a possible mechanism for signal transmission in pancreatic islets of langerhans. Biophys. J. **80**, 1195–1209 (2001)
5. Rocheleau, J.V., Walker, G.M., Head, W.S., McGuinness, O.P., Piston, D.W.: Microfluidic glucose stimulation reveals limited coordination of intracellular Ca^{2+} activity oscillations in pancreatic islets. Proc. Natl. Acad. Sci. U. S. A. **101**(12), 899–903 (2004)
6. Sherman, A.: Calcium and membrane potential oscillations in pancreatic β-cells. In: Othmer, H.G., Adler, F.R., Lewis, M.A., Dallon, J.C. (eds.) Case Studies in Mathematical Modelling: Ecology, Physiology, and Cell Biology, pp. 199–217. Prentice-Hall, New York (1997)
7. Pedersen, M.G.: Wave speeds of solutions to density dependent nonlinear nagumo diffusion equations—inspired by oscillating gap-junction conductance in the pancreatic islets of langerhans. J. Math. Biol. **80**, 683–698 (2005)
8. Keener, J.P.: Homogenization and propagation in the bistable equation. Physica D **136**, 1–17 (2000)
9. Scott, A.C.: Nonlinear Science. Emergence and Dynamics of Coherent Structures. Oxford University Press, New York (2003)